



Modelling long-term blanket peatland development in eastern Scotland.

Ward Swinnen^{1,2}, Nils Broothaerts¹, Gert Verstraeten¹

¹Department of Earth and Environmental Science, KU Leuven, Leuven, 3000, Belgium

5 ²Research Foundation Flanders - FWO, Brussels, 1000, Belgium

Correspondence to: Ward Swinnen (ward.swinnen@kuleuven.be)

Abstract. Blanket peatlands constitute a rare ecosystem on a global scale but is the most important peatland type on the British Isles. Most long-term peatland development models have focussed on peat bogs and high-latitude regions. Here, we present a spatially-explicit hillslope model to simulate long-term blanket peatland development along complex hillslope topographies.

10 To calibrate the model, the peatland architecture was reconstructed along 56 hillslope transects in the headwaters of the river Dee (633 km²) in eastern Scotland, resulting in a dataset of 866 soil profile descriptions. The application of the calibrated model using local pollen-based land cover and regional climate reconstructions over the last 12,000 years shows that the early-Holocene peatland development is largely driven by a temperature increase. An increase in woodland cover only has a slight positive effect on the peat growth potential contradicting the hypothesis that blanket peatland developed as a response to
15 deforestation. Both the hillslope measurements and the model simulations demonstrate that the blanket peatland cover in the study area is highly variable both in extent and peat thickness stressing the need for spatially distributed peatland modelling. At the landscape scale, blanket peatlands were an important atmospheric carbon sink during the period 9.5 ka – 6 ka BP. However, during the last six thousand years, the blanket peatlands are in a state of dynamic equilibrium with minor changes in the carbon balance.

20 **1 Introduction**

Peatlands occur across the globe and contain up to one third of the global soil carbon stock, despite covering approximately less than three percent of the Earth's surface (Gorham, 1991; Xu et al., 2018). Especially at higher latitudes, peatlands are an important ecosystem type and their dynamics have profoundly influenced the terrestrial carbon cycle throughout the Holocene (Yu et al., 2011). Unfortunately, little is known about long-term peatland dynamics and their response to climatic and land
25 cover changes (Wu, 2012).

Blanket peatlands are spreads of peat of varying thickness, covering the underlying topography, thus “blanketing” the landscape (Gallego-Sala et al., 2016). This peatland type occurs in hyperoceanic climates with cool and moist conditions throughout the year, and is mostly confined to the maritime edges of the continents (Gallego-sala and Prentice, 2013). Due to their location in the landscape, blanket peatland formation is more controlled by topography, compared to other peatland types



30 (Parry et al., 2012). Although rare on a global scale, up to 6 percent of the area of the United Kingdom is covered by blanket peatland (Jones et al., 2003). The large extent of the Scottish blanket peatlands, covering 23 percent of the land area, compared to the international rarity of these environments, make the Scottish peatlands of high conservation value (Fyfe et al., 2013; Tipping, 2008).

During the Holocene period, large areas of blanket peatland have developed throughout the Scottish Highlands and this shift
35 from mineral to waterlogged and nutrient-poor organic soils is one of the most important Holocene landscape changes in Scotland. Different hypotheses have been raised regarding the cause of this peatland development (Tipping, 2008). The original hypothesis, as proposed by Moore, linked the blanket peatland initiation to human impact, where anthropogenic land use change and increased grazing during the Neolithic period led to a shift in the hillslope hydrology resulting in the paludification of the upland soils (Moore, 1973). While this hypothesis has been supported by local studies throughout the British Isles, other
40 authors have suggested that, at least for Scotland, the initiation of blanket peatlands resulted from climatic changes during the Atlantic period (Ellis and Tallis, 2000; Huang, 2002; Simmons and Innes, 1988; Tipping, 2008). A recent study based on a database of basal radiocarbon dates shows regional differences in the timing of the blanket peatland development with an earlier timing for Central and Southern Scotland, compared to the other regions of the British Isles (Gallego-Sala et al., 2016). Most of the case studies studying the blanket peatland initiation are based on field data such as pollen cores and radiocarbon
45 dating, but studying causalities based on timing alone is difficult (Gallego-Sala et al., 2016). Process-based modelling of this landscape transformation could prove to be a useful technique, complementary to the field data, to provide insight in the underlying processes and mechanisms.

In recent decades, several peatland models have been developed, varying in spatial and temporal scale and in model complexity (Frolking et al., 2010). A good overview of the models developed for simulating long-term peatland behaviour is given by
50 Baird et al. (2012). Currently, several long-term peatland models such as Digibog and the Holocene Peatland Model (HPM) allow to simulate peatland processes and the feedbacks between ecology, hydrology and peat properties over Holocene timescales (Baird et al., 2012; Frolking et al., 2010). These models have been applied successfully within the context of peat bogs, but are difficult to transfer to blanket peatlands for two reasons. Firstly, these models are developed as cohort models, where each year, a new peat layer is added to the soil profile and included in the calculations for the remaining part of the
55 simulations. As a result, these allow to simulate temporal changes in peat properties such as hydraulic conductivity within the peat profile, but as the simulated time period increases, these models become computationally expensive, especially when a spatial dimension is added. As a result, they are difficult to apply to a landscape scale. Secondly, these models have been developed for peat bogs, which have a different peatland architecture compared to blanket peatlands and are therefore not always adapted to simulating peatland processes along complex hillslope topographies.

60 In this study, a long-term peatland model is presented which is able to simulate the hillslope hydrology and peatland dynamics along topographically complex hillslopes on Holocene timescales. Additionally, the representation of the model domain is relatively simple using a diplotelmic peat profile, making it computationally feasible to study peatland development on a landscape scale by simulating a large number of hillslope cross-sections. The model is applied to the Upper Dee catchment in



65 the Cairngorms National Park, eastern Scotland. The goal of this study is twofold. Firstly to apply a relatively simple process-based peatland model to study the long-term blanket peatland development in the Scottish Highlands on a landscape scale. Secondly, to identify the relative importance of climatic and land cover changes in the long-term blanket peatland development.

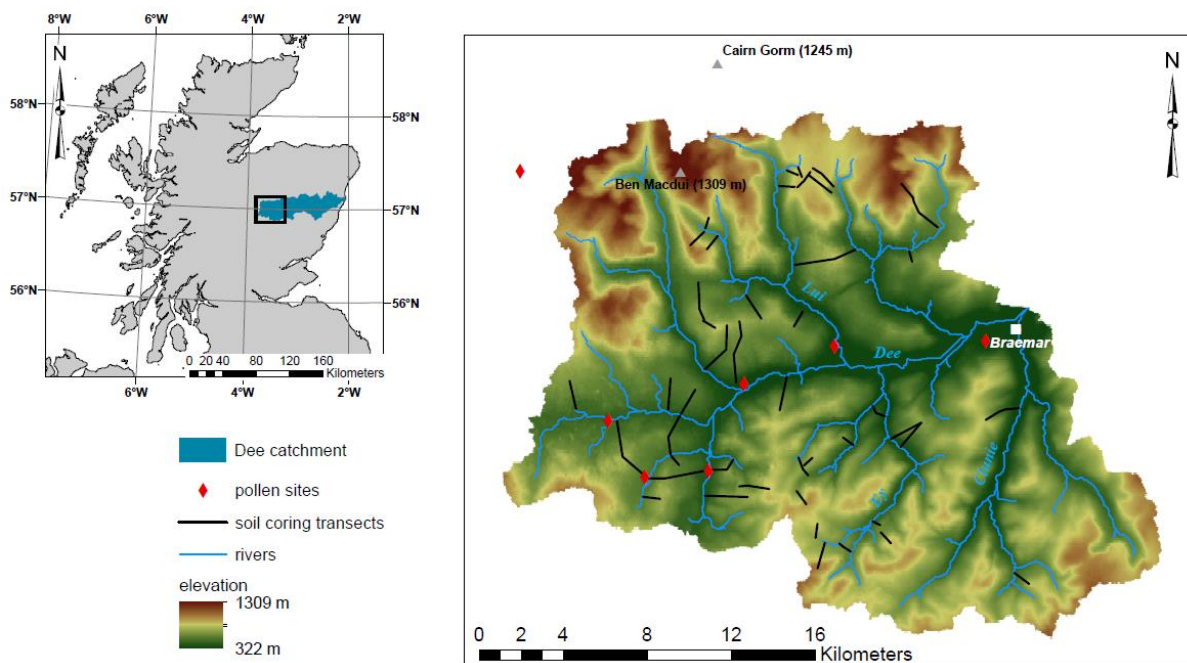
2 Materials and methods

2.1 Study area

70 The study area consists of the headwaters of the river Dee in eastern Scotland, with an elevation ranging from 322 to 1309 metres a.s.l. The area lies in the centre of the Cairngorms National Park and is managed by the Mar Lodge, Invercauld and Mar estates (fig.1). The geology of the Dee catchment is characterised by metamorphic and igneous rocks, with schists and granulites in the southern part of the study area and granite batholith intrusions in the north (Maizels, 1985). The entire area was glaciated by the Scottish ice sheet during the last ice age, which retreated between approximately 16 ka and 13.6 ka BP. In contrast to the Western Highlands, the Cairngorms massif was not subjected to widespread glacial expansion during the 75 Younger Dryas (Loch Lomond Stadial). During this period, the glacial activity remained largely restricted to the cirques (Everest and Kubik, 2006). The development of the current landscape and soils in the upper Dee area has been influenced by the deglaciation, forming a wide variety of glacial and fluvioglacial landforms (Ballantyne, 2008). In many parts of the study area, the bedrock is covered by glacial till of varying thickness (Maizels, 1985). The summits and ridges mostly carry skeletal soils and bedrock outcrops, while the slopes are covered by blanket peat and alpine podzols (Smith, 1985). The peat deposits 80 are found both lying directly on bedrock and overlying a layer of mineral sediment. This mineral substrate consists of gravel-rich silt loam and sandy loam in the southern part of the study area and sandy loam to loamy sand in the northern part.

Currently, the area is dominated by semi-natural land cover, including alpine and montane heath vegetation on the highest summits, heather moorland and small pockets of natural forest (Tetzlaff and Soulsby, 2008). The total annual precipitation ranges from 800 mm in the eastern part of the study area to almost 2000 mm on the mountain tops, with a significant proportion 85 of the precipitation falling as snow during the winter months (Dunn et al., 2001). The temperature regimes can vary considerably within the study area. The town of Braemar (339 m a.s.l.), has a mean annual temperature of 6.8 °C, ranging from 1.6 °C as a mean winter temperature (DJF) to 12.8 °C as a mean summer temperature (JJA). In contrast, the summit of Cairn Gorm (1245 m a.s.l.) has a mean annual temperature of 0.6 °C, and ranges from a mean winter temperature (DJF) of -2.6°C to a mean summer temperature (JJA) of 5.3 °C.

90 Early Holocene traces of human presence have been found within the study area, with archaeological evidence indicating the presence of Mesolithic hunter-gatherer structures as early as 8.2 ka cal BP in the western part of the study area (Warren et al., 2018). The first traces of permanent settlement in the Upper Dee are from the village of Braemar around 1000 AD (Paterson, 2011). In contrast to the western part of Scotland, the study area shows no traces of large scale peat extraction, which is probably due to the relatively thin peat profiles and difficult access to the area (Maurer, 2015).



95

Figure 1: Location of the Upper Dee catchment, with indication of the hillslope transects and the pollen sites used for the land cover reconstruction.

2.2 Field data

For the study area, the blanket peatland architecture was reconstructed along 56 hillslope transects across the study area during field campaigns in 2015 and 2017 (fig. 1). Soil corings were made along the transects with a spacing of approximately 50 metres using a gauge auger. The hillslope topography was measured using Post-Processing RTK GPS measurements. The transect locations were selected in order to include a wide variety of lithologies, elevation zones and topographic parameters such as aspect, slope and curvature. Additionally, the carbon content, dry bulk density and water content of the peat deposits were derived from field samples, collected as core sections with a length of 5 centimetres. The regional vegetation evolution over the past 12,000 years was reconstructed based on seven pollen cores located within the study area (fig. 1). These cores provide vegetation information from different elevation zones and with a varying distance to the low-lying valleys of the Dee and the Spey (Birks, 1969; Hunter, 2016; Huntley, 1994; Paterson, 2011). Using the REVEALS model (Regional Estimates of Vegetation Abundance from Large Sites (Sugita, 2007)), the pollen percentages were converted to regional vegetation fractions. REVEALS was developed to reconstruct regional vegetation composition using pollen data from large lakes, but previous studies has shown that a group of sites can also be used to estimate regional vegetation using REVEALS (Fyfe et al., 2013; Mazier et al., 2012; Trondman et al., 2016). Pollen type parameters (pollen productivity and fall speed) were based on the standardized set of Mazier et al., (2012). The regional vegetation fractions were grouped in five classes (coniferous trees, deciduous trees, shrubs, heather, grasses & herbs) and used as land cover input in the hillslope model. As the land cover

105
110

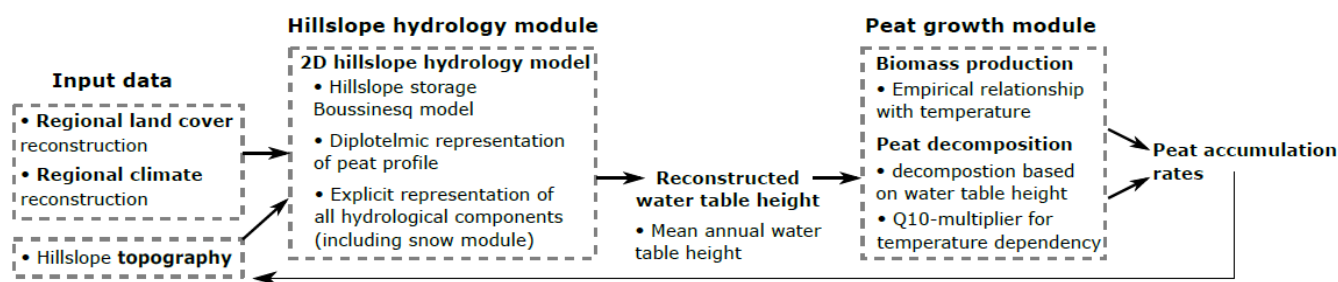


reconstruction for Scotland based on REVEALS by Fyfe et al. does not include pollen data from high-elevation sites, a new
 115 land cover reconstruction was made by Hunter (2016) for this study using local pollen data (Fyfe et al., 2013; Hunter, 2016).
 At all coring locations, the soil profiles were described based on visual inspection, analysing the colour, texture and possible
 presence of macroscopic remains (charcoal, wood, ...). Based on the coring descriptions, the peat thickness could be derived.
 In this study, peat is defined as a dark organic-rich layer of minimal 10 centimetres thick without or with minimal presence of
 120 mineral material based on visual inspection. Organic-rich horizons with a clear presence of mineral material were not classified
 as peat.

In total, 34 peat samples were radiocarbon dated at 17 locations throughout the study area, encompassing a range of topographic
 situations and peat thicknesses (see appendix A2 for dating details). All radiocarbon dates were performed by the Belgian
 Royal Institute for Cultural Heritage and calibrated using the Oxcal 4.3 software and the IntCal13 calibration curve (Bronk
 Ramsey, 2009; Reimer et al., 2013).

125 2.3 Model outline

The basic structure of the hillslope peatland model consists of a hydrology module simulating the water table behaviour along
 the hillslope, which is coupled to a peat growth module simulating biomass production and peat decomposition (fig. 2). The
 model domain consists of a two-dimensional hillslope cross-section, which is discretised in a series of model gridpoints. The
 stratigraphy consists of an impermeable bedrock, overlain by a layer of glacial till. Over time, a peat profile can develop on
 130 top of this mineral substrate when the right environmental conditions are met locally. To enable the use of the Boussinesq-
 equation for the simulation of the hillslope hydrology, local topographic depressions are filtered out. The hillslope topography
 is based on the detailed GPS-measurements for each coring location.



135 **Figure 2: General model workflow. For a more detailed description of the model structure, the reader is referred to the text.**

2.3.1 Hillslope hydrology module

The water table dynamics are modelled using a variant on the Boussinesq equation for a non-constant slope (Hilberts et al., 2004):

$$\text{Eq. (1)} \quad \varepsilon \frac{\partial S}{\partial t} = \frac{k}{\varepsilon} \cos i(x) \left[B \frac{\partial S}{\partial x} + S \frac{\partial B}{\partial x} + \varepsilon S \frac{\partial i(x)}{\partial x} \right] + \frac{k}{\varepsilon} \sin i(x) \left[\varepsilon \frac{\partial S}{\partial x} - SB \frac{\partial i(x)}{\partial x} \right] + \varepsilon N$$



140 With $B = \frac{\partial}{\partial x} S$

With x the distance to the hillslope bottom (m), ε the soil porosity (m m^{-1}), S the actual water storage (m), k the hydraulic conductivity (m s^{-1}), i the bedrock slope (m m^{-1}) and N the rainfall recharge or infiltration (m) (Hilberts et al., 2004). Given the shallow position of the water table in blanket peatlands, the unsaturated zone is excluded from the hydrological calculations, assuming an instantaneous exchange (e.g. infiltration and evapotranspiration) between the surface and the saturated zone of
145 the soil profile. As a result, the computational time is significantly reduced (Ballard et al., 2011).

The diplotelmic nature of the model is represented by the depth-integrated saturated hydraulic conductivity. Each stratigraphic unit (mineral substrate, catotelm and acrotelm) has a specific saturated hydraulic conductivity value.

A simple snow module is included in the hydrological model, with precipitation falling as snow during periods with sub-zero temperatures. The amount of melt is based on a degree day factor model. For each timestep, infiltration- and saturation excess
150 overland flow is calculated. The produced runoff is assumed to leave the hillslope before the next timestep. For open peatland vegetation types, all rainfall is assumed to be able to infiltrate for intensities below 2 mm h^{-1} . For higher intensities, the infiltration rate increases with higher precipitation rates:

$$\text{Eq. (2)} \quad ir = 0.626 * p + 0.0002$$

With ir the infiltration rate (mm h^{-1}), p the precipitation rate (mm h^{-1}) (Holden and Burt, 2002). For woodland peatlands,
155 infiltration rates of up to 30 mm h^{-1} are reported (Cairns et al., 1978). In the model, this maximal infiltration rate of 30 mm h^{-1} is used for a fully forested peatland. The final infiltration rate at a certain location is determined based on linear interpolation between the infiltration rates of open and forested peatland based on the percentage woodland cover at each model gridpoint. The potential plant transpiration and soil evaporation (mm day^{-1}) are calculated separately based on the Leaf Area Index (LAI), which enables differentiation based on the vegetation cover (eq. (3)) (Williams et al., 1983).

$$160 \text{ Eq. (3)} \quad E_{soil} = E_{pot} e^{(-0.4LAI)}$$

$$E_{plant} = \frac{E_{pot} LAI}{3}, 0 \leq LAI \leq 3$$

$$E_{plant} = E_{pot} - E_{soil}, LAI > 3$$

With E_{soil} the soil evaporation rate (mm day^{-1}), E_{plant} the plant transpiration rate (mm day^{-1}) and E_{pot} the potential evapotranspiration rate (mm day^{-1}), which is calculated using the Thornthwaite equation based on the mean monthly
165 temperature.

The actual evapotranspiration rate (AET) (mm day^{-1}) is calculated as a function of the water table depth (eq. (4)). If a gridpoint consists of glacial till without a peat cover, the AET is at the potential rate when the water table is at the surface ($z_1 = 0$) and decreases linear until depth z_2 . If peat is present, the actual evapotranspiration is assumed to be at the potential rate if the water table is located in the upper horizon ($z_1 = \text{acrotelm thickness}$) and decreases linearly until a depth z_2 (m) (Frolking et al., 2010;
170 Lafleur et al., 2005).

$$\text{Eq. (4)} \quad AET_t = \left(E_{soil} + E_{plant} \right) \frac{z_2 - wt}{z_2 - z_1}, \text{ for } z_1 \leq wt \leq z_2$$



Input data for temperature and precipitation values are based on a European gridded dataset of mean annual temperature and mean monthly precipitation anomalies for the last 12,000 years derived from pollen data (fig. 3) (Mauri et al., 2015). As total annual precipitation amounts and mean annual temperatures vary considerably throughout the study area, the precipitation and temperature data were corrected for orographic effects. Data from eight meteorological stations in the vicinity of the study area were used to construct linear regression models, correcting the mean daily precipitation amount and mean annual temperature for each location based on the elevation (eq. (5) – eq. (6)) (see appendix A1 for the weather station details):

$$\text{Eq. (5)} \quad P = (0.003776 * E) + 1.669$$

$$\text{Eq. (6)} \quad MAT = (-0.0083 * E) + 13.2839$$

With P the mean daily precipitation amount (mm), E the elevation (m a.s.l.) and MAT the mean annual temperature ($^{\circ}\text{C}$). The time series used as model input are based on daily temperature and hourly precipitation data from the weather station of Braemar, which are rescaled using both the regression equations for elevation effects and the long-term anomalies for temperature and precipitation (fig. 3). As a result, precipitation and temperature series with a high temporal resolution are used throughout the entire studied period. The model is run with a spatial resolution of 50 metres, similar to the average coring distance. The time resolution is set to 400 seconds for the hillslope hydrology module and 1 year for the peat growth module to ensure model stability.

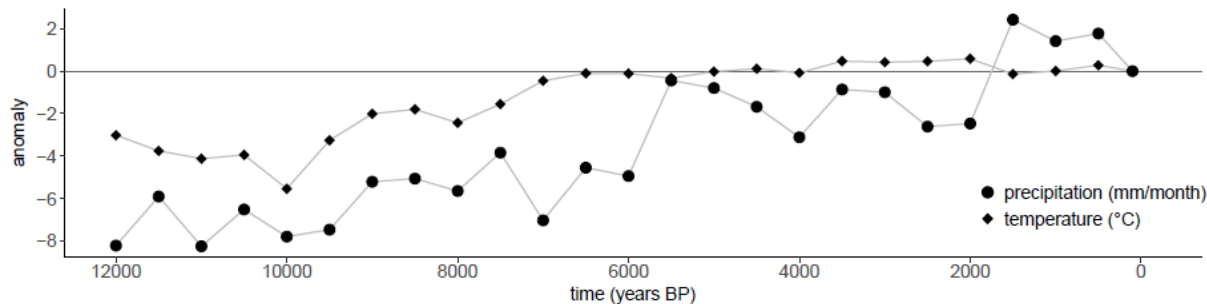


Figure 3: Reconstructed mean annual temperature ($^{\circ}\text{C}$) and mean monthly precipitation (mm month^{-1}) anomalies for the period 12 ka – 100 BP with a 500-year interval for the location of Braemar. Values extracted from a gridded European dataset with a spatial resolution of 1x1 degree (Mauri et al., 2015).

2.3.2 Peat growth module

The peat accumulation at each gridpoint is calculated as the balance between biomass production and decomposition. The biomass production is simulated using a power function regression equation based on field data for the Moor House Reserve (Garnett, 1998), corrected for the woodland cover.

$$\text{Eq. (7)} \quad NPP = 60.06 (MAT^{1.134}) * (1 + (\frac{wc}{wc_{max}} * wi))$$

With NPP the Net Primary Production ($\text{g m}^{-2} \text{a}^{-1}$), MAT the mean annual temperature at the gridpoint location ($^{\circ}\text{C}$), wc , the woodland fraction, wc_{max} the woodland percentage of a fully forested peatland and wi the percentage increase in NPP between an open and wooded peatland. In general, the NPP is higher for wooded peatland compared to open peatland vegetation, with



reported values of a 12 percent increase for bogs and 17 percent for fens (Beilman and Yu, 2001; Szumigalski and Bayley, 200 1997). In this study, w_i is set to 15 percent and $w_{C_{max}}$ to 40 percent.

The peat column at each gridpoint is divided in an oxic and anoxic zone based on the calculated mean annual water table height. The total decomposition can thus be written as:

$$\text{Eq. (8)} \quad D = k_1 * wt + k_2 * (h - wt)$$

With D the total decomposition (m a^{-1}), k_1 and k_2 the rates of decomposition under anoxic and oxic conditions (yr^{-1}), h the 205 thickness of the soil profile above the bedrock (m) and wt the height of the water table above the bedrock (m) (Hilbert et al., 2000). The decomposition rates are dependent on the mean annual air temperature using a Q_{10} -temperature multiplier, which is the ratio by which the biomass respiration rate increases under a 10 °C temperature increase. As the Q_{10} -value itself is assumed to be temperature dependent, two values are used in this study. A Q_{10} -value of 2.2 is used for temperatures above 5 °C, and 3.7 for temperatures between -4 and 5 °C. Below -4°C, the decomposition is assumed to cease completely (Chapman 210 and Thurlow, 1998; Rosswall, 1973 as cited by Clymo, 1984; Wu, 2012). The biological module runs at an annual timescale. Based on the calculated peat accumulation rate, the hillslope topography is updated annually.

2.3.3 Peatland initiation

Simulations start with a hillslope consisting of an impermeable bedrock covered by glacial till. As the thickness of the till is not known at each location, it is assumed to have a constant thickness of 50 centimetres. Over time, the organic matter 215 accumulates within the upper 30 centimetres of the mineral soil forming an organic-rich horizon based on the balance between biomass production and decomposition. When a threshold is exceeded (in this case the amount of organic matter equivalent to a peat layer of 10 centimetres), additional organic matter which is produced, starts to accumulate as peat at that location, with the properties of an acrotelm. This ensures that a similar definition for peat is used both for the hillslope corings as for the model simulations. Once the peat thickness exceeds the thickness of the acrotelm layer, the peat layer becomes diplotelmic, 220 with the peat below the acrotelm having the properties of the catotelm. Once the biomass within the simulated peat profile decreases below the biomass threshold, the gridpoint is no longer considered to be covered by a peat layer and only mineral soil properties are taken into account.

2.3.4 Boundary conditions

The impermeable bedrock below the glacial till is used as a zero-flux boundary condition at the bottom of the model domain. 225 At several locations throughout the study area, rivers have eroded the stream bank, exposing the peat. At the lower end of the hillslope, the water storage is thus set to a fixed value, representing the depth of the river. For the gridpoint at the top of the hillslope transect, a lateral zero-flux boundary is assumed.



2.4 Model calibration and validation

Model calibration is based on the measured mean peat thickness per topographic class. In total, nine topographic classes were defined by dividing both the measured slope and curvature at each coring location in three classes, resulting in nine possible combinations. The calibration procedure resulted in topographic class limits of 0.098 and 0.135 m m⁻¹ for slope and -0.184*10⁻³ m⁻¹ and 0.184*10⁻³ m⁻¹ for curvature. For all 56 hillslope transects, the modelled mean peat thickness per topographic class after 12,000 years of simulation is compared to the mean peat thickness measured in the field. In total, three model parameters were calibrated: the decomposition rates under oxic and anoxic conditions and the acrotelm thickness. The goodness-of-fit of each parameter combination was evaluated based on minimization of the Root Mean Squared Error (RMSE) between the mean modelled and measured peat thickness per topographic class. Out of the 866 hillslope corings, 433 were selected randomly to be used as calibration points and the others as validation points. Since the spacing between the soil corings is slightly variable, the model results were resampled to the locations of the soil corings using linear interpolation.

As an additional validation of the model behaviour, the simulated peat growth initiation dates for all model gridpoints can be evaluated against a dataset of basal radiocarbon dates for blanket peat deposits in the upland regions of Scotland, with an elevation above 300 metres a.s.l. (n = 30) (Gallego-Sala et al., 2016). The dataset was expanded by incorporating 17 additional basal radiocarbon dates on peat deposits from within the study area (see appendix A2 for dating details). For each of the 17 locations within the study area for which radiocarbon dates were available, the basal age was estimated using the clam 2.2 software package to construct age-depth models and extrapolate to the bottom of the peat layer (Blaauw, 2010). As the available initiation dates based on radiocarbon dating were not necessarily taken at the modelled transect locations, the comparison between modelled and observed peat growth initiation is based on the probability density curves using a bin width of 500 years. Depending on the amount of available radiocarbon dates at each location, some estimates of the peat growth initiation date were based on the extrapolation of the age-depth model over large sections of the peat profile. To analyse the effect of the age-depth model extrapolation on the resultant probability density curve, an additional probability density curve was constructed containing only those radiocarbon dated samples which were directly measured at the bottom of a peat layer (n = 20).

3 Results

3.1 Field measurements

Based on the definition of peat used in this study, 57 percent of the coring locations contained a surface peat layer, with a mean measured peat thickness over all coring locations of 36 centimetres, with a maximal value of 3 metres. The mean measured peat thickness per hillslope transect varies between 0 and 96 centimetres (fig. 4). Overall, the transects with a high mean peat thickness can be found in the upstream parts of tributaries of the river Dee. Strong spatial variability occurs, even at small distances, making the peat cover throughout the area highly variable in both occurrence and mean thickness. The mean



measured peat thickness per topographic class ranges from 23.6 ± 31.9 cm for the class with a moderate slope and a convex curvature to 54.1 ± 65.3 cm for the topographic class with a low slope and a straight curvature. Based on 35 randomly selected soil samples, which were identified in the field as peat, the median organic carbon percentage was calculated at 51.9 ± 7.3 percent and the dry bulk density at 127.5 ± 63.2 kg m⁻³.

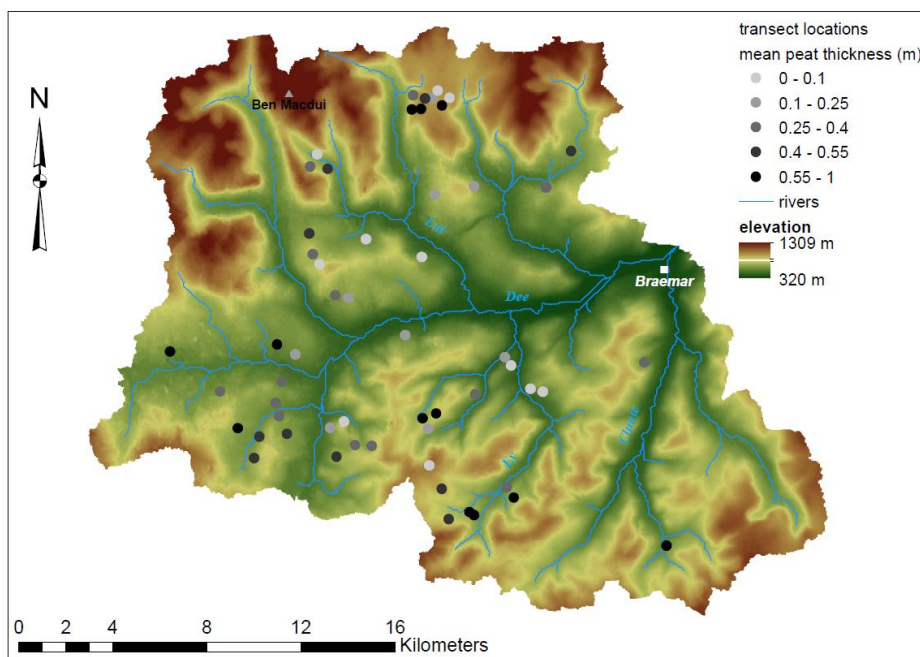


Figure 4: Mean measured peat thickness per hillslope transects (n = 56).

265

The pollen-based reconstructed land cover shows an early-Holocene woodland increase until the period 8.4 ka - 7.2 ka cal BP (fig. 5). This period is followed by a general woodland decline, with the woodland cover dropping below 5 percent from 3.6 ka cal BP onwards. The reconstructions for the individual pollen cores show an important east-west gradient in terms of maximal forest cover, with higher woodland percentages for the eastern and lower-lying part of the study area (Paterson, 2011).

270

The woodland is of a mixed type containing both coniferous species (Scots pine) and deciduous species (birch, rowan and aspen). A study by Fyfe et al., reconstructed the Holocene vegetation over Scotland using the REVEALS model for seven sites across the Scottish mainland, resulting in a maximal forest extent by 6.7 ka cal BP (Fyfe et al., 2013). The data presented here show an earlier woodland cover decline around 7.2 ka cal BP and a larger proportion of coniferous species in the forest composition. In comparison to the sites of Fyfe et al., the woodland cover shows to be relatively low, with an open heather

275

landscape prevailing during the period under study, which can be attributed to the relatively high elevation of the study area.

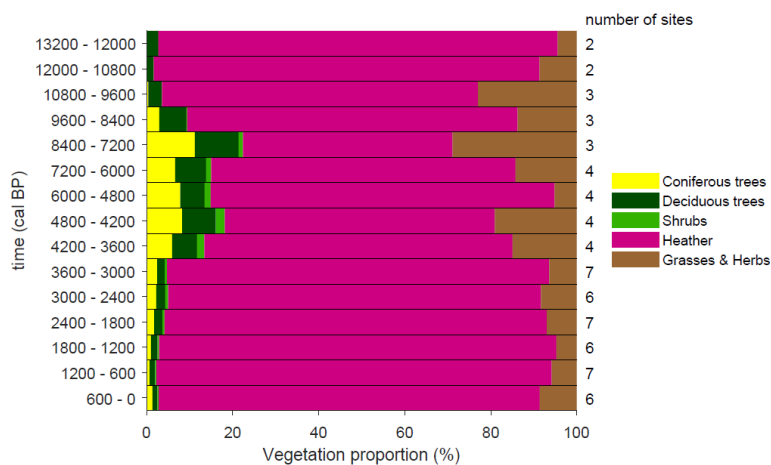


Figure 5: Reconstructed vegetation proportions for the study area using the REVEALS model, based on seven pollen cores.

3.2 Model calibration

Point-by-point calibration resulted in poor correspondence between the modelled and observed peat thickness. As a consequence, the model parameters were calibrated based on the mean peat thickness per topographic class. In total, nine topographic classes were constructed by classifying all coring locations based on the slope and the hillslope curvature. The best fitting parameter combination results in an acrotelm thickness of 10 centimetres, an oxic decomposition rate at 10°C of 2.15 percent year⁻¹ and an anoxic decomposition rate at 10°C of 0.24 percent year⁻¹, which corresponds to an oxic/anoxic decomposition ratio of 9. These values correspond largely to those reported in the literature (Ballard et al., 2011; Clymo, 1984; Wu, 2012; Yu et al., 2001). The RMSE on the mean peat thickness for the best fitting parameter combination is 9.53 centimetres (fig. 6).

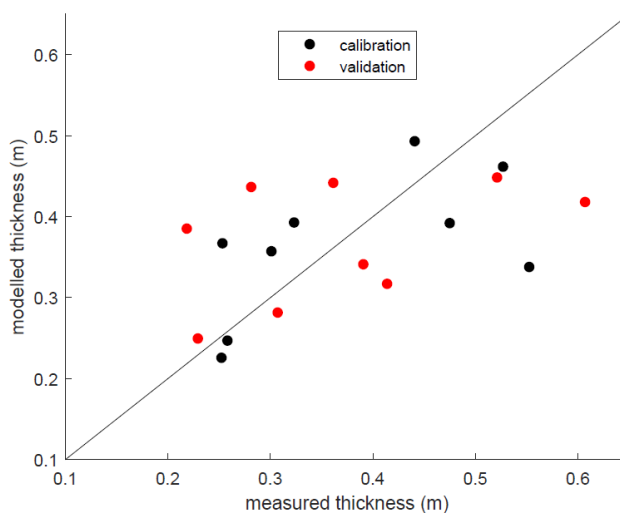
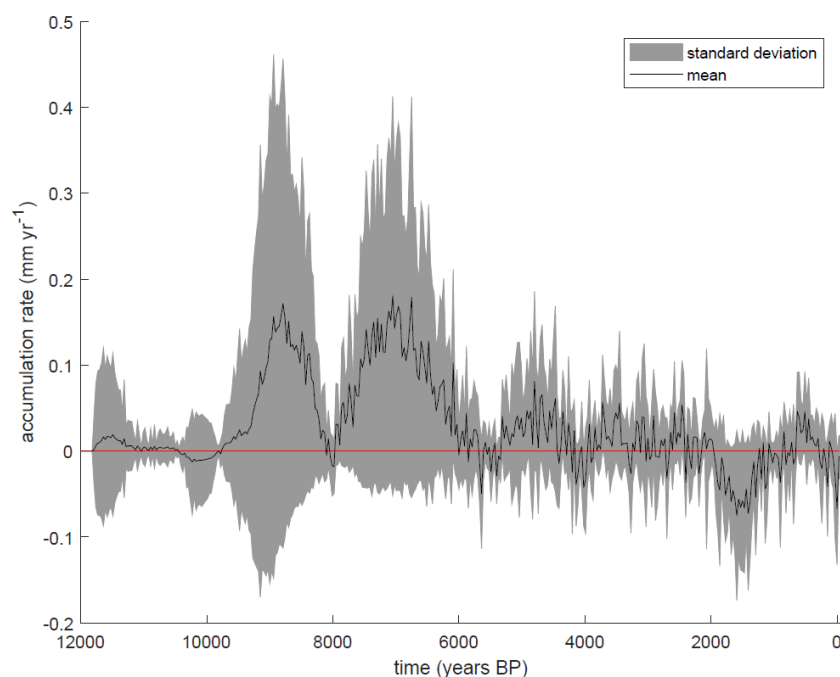


Figure 6: Modelled and measured mean peat thickness per topographic class for both the calibration and validation transects.



3.3 blanket peatland development

290 The calibrated model was run to simulate the long-term blanket peatland development since 12 ka BP for the 56 hillslope
transects using the calibrated parameter values. The reconstructed land cover history (fig. 5) is used as vegetation evolution
throughout the simulations. Overall, the model simulations indicate that mean peat accumulation rates were low until 9.5 ka
BP, with small variations between the different gridpoints (fig. 7). Later, the accumulation rates increased and were high during
two phases in the early Holocene, 9.5 – 8.5 ka BP and 8 – 6.5 ka BP. From 6 ka BP to 2 ka BP, the rates were relatively stable
295 and slightly positive on average. A long-term decrease in accumulation rates occurred between 2 ka BP and 1 ka BP, which
increased again to positive values around 0.5 ka BP. The mean peat and carbon accumulation rate over all gridpoints and for
the entire studied period is $0.03 \cdot 10^{-3} \text{ m year}^{-1}$ and $1.79 \text{ g C m}^{-2} \text{ year}^{-1}$. The maximal mean peat and carbon accumulation rate
over the entire studied period is $0.18 \cdot 10^{-3} \text{ m year}^{-1}$ and $11.95 \text{ g C m}^{-2} \text{ year}^{-1}$ and occurs at 7050 years BP.



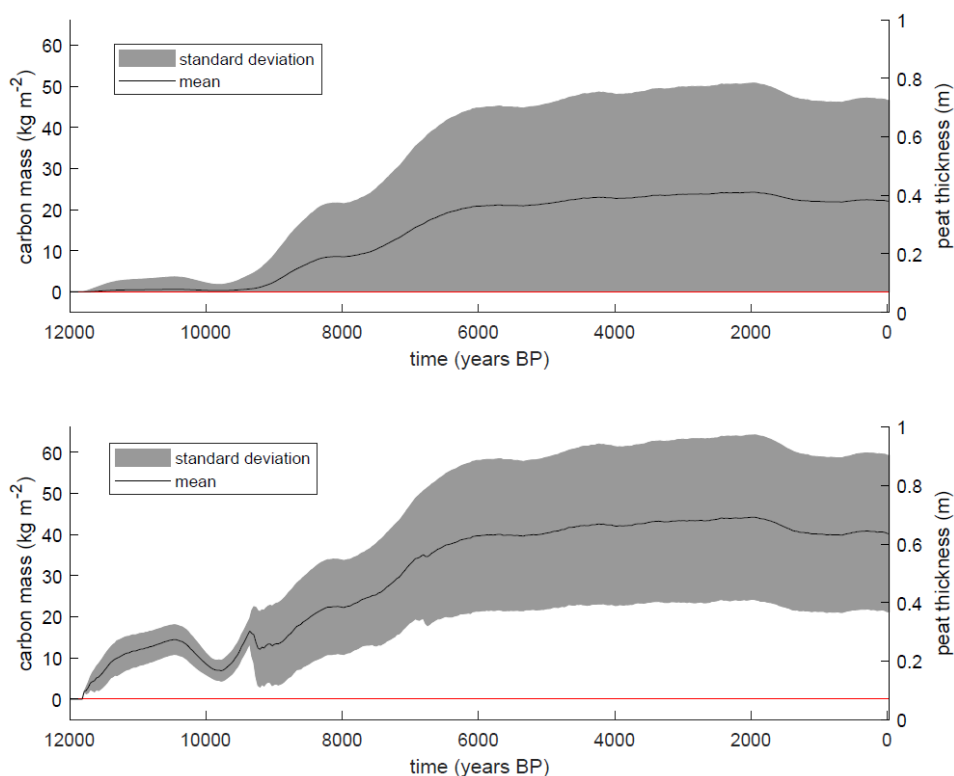
300

Figure 7: Simulated mean peat accumulation rate and standard deviation for all studied hillslope transects (n = 56).

Figure 8 indicates the evolution of the mean peat thickness and corresponding organic carbon mass over all hillslope transects.
The mean peat thickness reaches a maximal value of 0.36 metres around 2 ka BP and declines slightly afterwards to a current
value of 0.33 metres or $22.04 \text{ kg C m}^{-2}$. Overall, the peatland development occurs mostly before 6 ka BP and shows limited
305 variations afterwards, with a slight decline in mean peat thickness between 2 ka BP and 1 ka BP. When only the model
gridpoints with a peat cover are considered, the maximal value for the modelled mean thickness is 0.66 metres, declining to

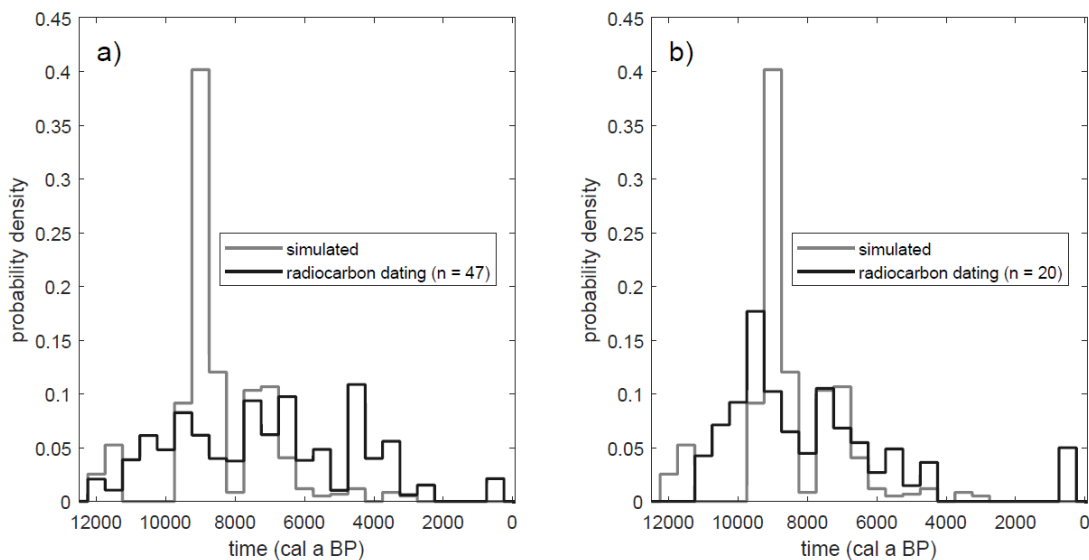


0.61 metres nowadays or $40.25 \text{ kg C m}^{-2}$. In total, the model simulates a peat cover at 61 percent of the coring locations, which is comparable to the coring data, which result in 57 percent peat cover.



310 **Figure 8: Simulated mean peat thickness/carbon mass and standard deviation for all gridpoints (top) and for the gridpoints with a**
315 **peat cover (bottom).**

Although the model calibration is solely based on the current peat thickness, the timing of peatland development can be evaluated based on radiocarbon dating of peat profiles. Overall, the model simulations indicate that peat growth initiated at most locations between 9.75 ka BP and 6.75 ka BP. The basal radiocarbon dates ($n = 47$) show a more diffuse pattern for the
315 Scottish upland areas (fig. 9a). When only considering those dates for which the radiocarbon sample was taken at the bottom of the peat column ($n = 20$), excluding the sites for which the initiation date was estimated by the extrapolation of an age-depth model to the bottom of the peat core, the probability density function shifts to older initiation ages and corresponds much better with the simulated dates (fig. 9b).



320 **Figure 9: Probability density function of the peat growth initiation dates based on the model simulation and the radiocarbon dating database for Scottish upland areas (above 300 metres a.s.l., see appendix A2) using a bin width of 500 years. a) all dates. b) All dates, excluding those for which a date was obtained by extrapolating an age-depth model to the bottom of the peat column.**

3.4 Sensitivity analysis

To study the model sensitivity to variations in parameter values a sensitivity analysis is carried out. In total, seven parameters are varied over the range as mentioned in the literature. The parameters broadly cluster in two groups, peat properties and environmental parameters (Table 1). Each parameter is varied stepwise, while all other parameters are kept at the standard value. The sensitivity is evaluated as the current mean peat thickness over all gridpoints after a simulation over a 12,000 year-period using the pollen-based climate and land cover variations as environmental boundary conditions (fig. 10). Overall, the model shows to be most sensitive to the peat decomposition rate, mean annual temperature and woodland cover. The peat thickness shows no sensitivity towards changes in catotelm conductivity, probably, because the low conductivity values of the catotelm anyhow result in slow drainage compared to other components of the hillslope hydrology and thus in quasi permanent water saturation of the catotelm. The acrotelm conductivity shows the same behaviour except for the lowest value. The acrotelm is under oxic conditions for most of the simulated values. Only for the lowest conductivity value, the water table rises above the catotelm-acrotelm boundary, resulting in lower decomposition rates and a higher mean peat thickness.

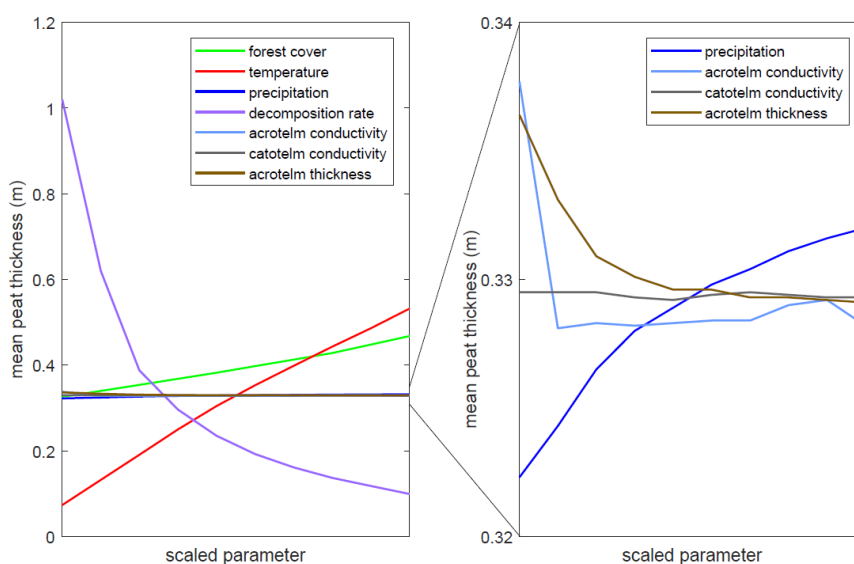
335

Table 1: Overview of the parameters used in the parameter sensitivity test, listing the standard value and the range over which the parameter is changed.

Parameter	Standard value	Minimum value	Maximum value	References
Peat properties				



Acrotelm saturated hydraulic conductivity (m s^{-1})	$1 \cdot 10^{-3}$	$1 \cdot 10^{-5}$	$1 \cdot 10^{-2}$	(Cunliffe et al., 2013; Holden et al., 2011; Ingram, 1983)
Catotelm saturated hydraulic conductivity (m s^{-1})	$1 \cdot 10^{-6}$	$1 \cdot 10^{-9}$	$3 \cdot 10^{-6}$	(Cunliffe et al., 2013; Dai and Sparling, 1973; Holden and Burt, 2003; Ingram, 1983; Rosa and Larocque, 2008)
Acrotelm thickness (m)	0.1	0.05	0.5	(Ballard et al., 2011; Belyea and Malmer, 2004; Clymo, 1984)
Oxic decomposition rate at 10°C ($\% \text{ yr}^{-1}$)	2.15	1	5	(Kleinen et al., 2012; Lucchese et al., 2010; Malmer and Wallen, 2004; Wu, 2012; Yu et al., 2001)
Environmental parameters				
woodland cover (%)	REVEALS-based land cover reconstruction (fig. 5)	0	100	(Hunter, 2016)
Mean annual temperature ($^\circ\text{C}$)	6.2	-50%	+50%	Standard value based on the mean annual temperature for Braemar for the period 1890 – 1919 (earliest data available) (MetOffice, 2012)
Mean annual precipitation (mm yr^{-1})	900	-75%	+75%	Standard value based on the mean annual precipitation for Braemar for the period 1890 – 1919 (earliest data available) (MetOffice, 2012)



340 **Figure 10: Mean simulated peat thickness for all variables used in the parameter sensitivity test.**



The climate sensitivity of a model gridpoint appears to be dependent on the presence of a peat layer. Overall, the percentage of model gridpoints covered by peat shows to be more sensitive to precipitation changes than the mean peat thickness (fig. 11, fig. 12). This might be a result of the diplotelmic representation of the peat profile. The strong difference in saturated hydraulic conductivity for the two peat horizons results in minimal water table changes when the precipitation amount is varied. In other words, the use of a diplotelmic model results in a water table which fluctuates only slightly around the acrotelm-catotelm boundary. As a result, the peat accumulation rates and resulting peat thickness are not very sensitive to precipitation changes. For the substrate, only a single saturated hydraulic conductivity value is used, which results in a more sensitive response to precipitation changes for the gridpoints which do not have a peat cover. Overall, the highest peat thickness and percentage peat cover can be found for the scenarios with a high temperature and precipitation amount.

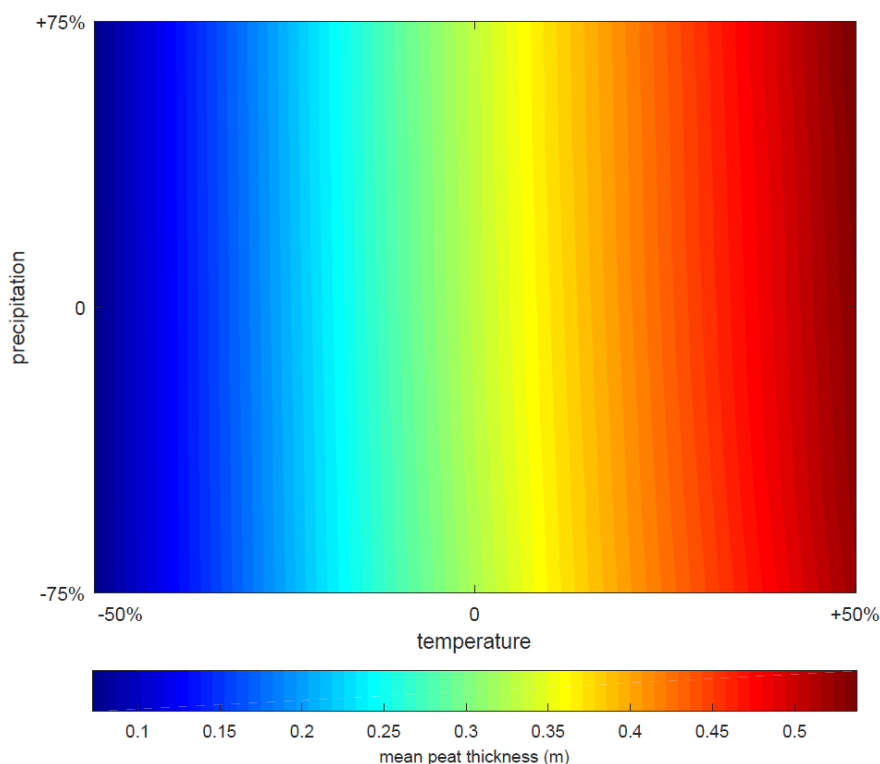
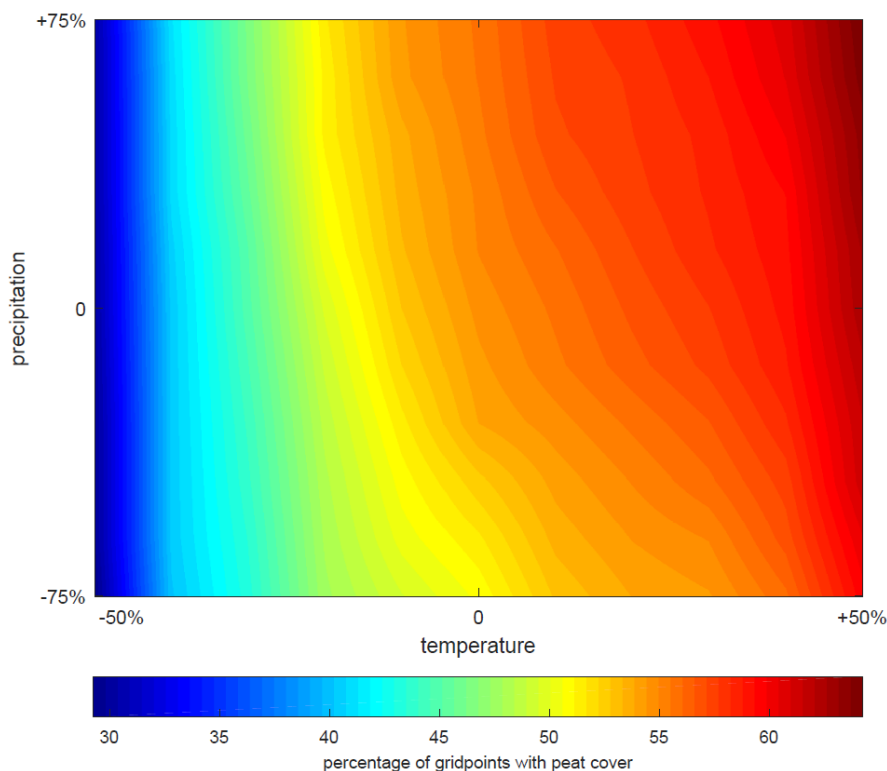


Figure 11: Mean peat thickness for all combinations of temperature and precipitation changes.



355 **Figure 12: Percentage of all model gridpoints with a peat cover of at least 10 centimetres for all combinations of precipitation and temperature variations.**

4 Discussion

Point-by-point calibration of the hillslope model resulted in a poor correspondence between modelled and observed peat thickness. Using the mean peat thickness per topographic class however allowed to calibrate the model with a RMSE below
360 10 centimetres (fig. 6). This indicates that a spatial peatland model with a simplified representation of the peat profile is unable to capture the local variability, but can replicate the general peatland evolution on the landscape scale. Similar model behaviour has been found in sediment erosion modelling, where point-by-point comparison yield poor correspondence but where the mean value per topographic class performs sufficiently well (Peeters et al., 2006). Overall, the peatland model is not able to simulate the high peat thickness values (larger than 1.5 metres), observed at some locations in the landscape, due to the
365 relatively high calibrated decomposition rates (fig. 13). This high rate can be attributed to two processes. Firstly the fact that the decomposition rate within the model does not only encompass peat decomposition within the soil profile, but also other processes which lead to decrease in peat thickness in the field such as particulate organic carbon export through gully development and shallow mass movements. These processes are not represented in the model but affect the peat thickness as it is measured in the field, leading to higher decomposition rates in the model calibration. Secondly, local depressions within
370 the hillslope topography were filtered out to enable the use of the Boussinesq-equation for the simulation of the subsurface



flow. Since local depressions showed to contain thick peat deposits in the field, the filtering procedure on the hillslope topography reduces the potential of modelling high peat thickness values at these locations.

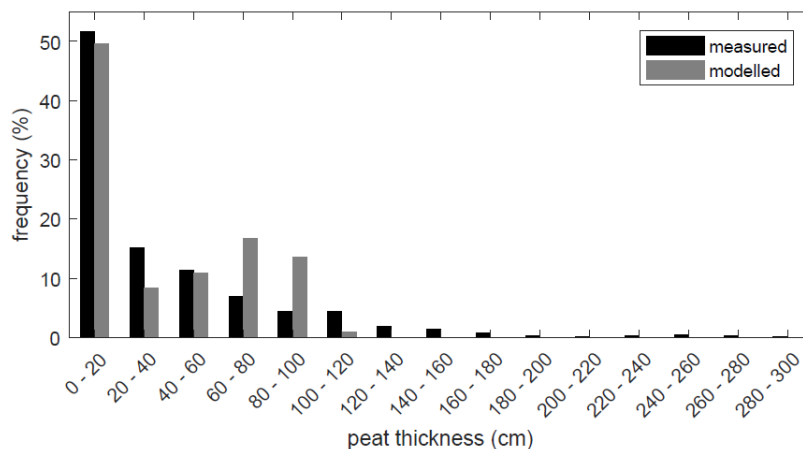


Figure 13: Frequency distribution of the measured and modelled peat thickness for all studied hillslope transects (n = 56).

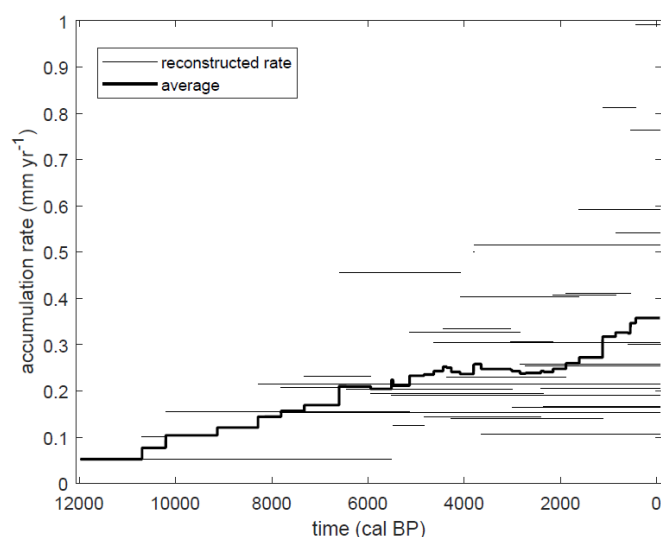
375 The range of simulated peat accumulation rates shows to be realistic, with periods of high mean accumulation rates coinciding with periods of temperature increase (fig. 3, fig. 7). More specific, the mean peat accumulation rates were high during the periods 10 ka – 8.5 ka BP where the mean annual temperature increased with 3.74°C, resulting in a mean peat accumulation rate over all modelled locations for the entire period of $0.064 \cdot 10^{-3} \text{ m yr}^{-1}$ or $4.24 \text{ g C m}^{-2} \text{ yr}^{-1}$ and 8 ka – 6.5 ka BP, with a temperature increase of 2.34°C and a mean peat accumulation rate of $0.104 \cdot 10^{-3} \text{ m yr}^{-1}$ or $6.88 \text{ g C m}^{-2} \text{ yr}^{-1}$. It appears to be
380 the temperature increase, rather than the temperature itself, which drives peat growth. The increased biomass production due to the temperature increase outweighs the lowering in water table height caused by higher evapotranspiration rates and creates an imbalance between production and decomposition, leading to positive accumulation rates and a peat thickness increase. In contrast to existing cohort models, which have shown to be capable of capturing local variations in dynamics within the peat profile, the relatively simple diplotelmic model presented here cannot reproduce the local dynamics with the same degree
385 of detail (Frolking et al., 2010; Morris et al., 2012). However, the simple representation of the model domain leads to a decrease in computation time which allows the application of the model over large spatial and temporal domains. In combination with the pollen-based climate and land cover reconstructions, it allows to study peatland development on the landscape scale, rather than at the scale of a single peat bog or peat profile as is often the case for the cohort models, allowing to answer different research questions.

390 **4.1 Peat growth initiation**

Based on the model simulations, the peat growth initiation dates cluster mostly within the period 9.75 ka – 6.25 ka BP (fig. 9), which corresponds largely to the Atlantic period, which is mentioned by other studies based on field data (Ellis and Tallis, 2000; Tipping, 2008). The database of basal radiocarbon dates shows a wider spread of initiation dates for upland Scotland



395 between 12.25 ka BP and 3.25 ka BP. However, a majority of the available basal dates within the dataset is based on a radiocarbon dating higher in the peat profile, which is extrapolated to the bottom of the core using an age-depth model. One could question whether this extrapolation is justified. The deeper parts of the peat profile are older and as a result, a smaller fraction of the originally deposited biomass will remain. This leads to lower reconstructed accumulation rates further back in time. The reconstructed rates based on the available radiocarbon dates for the study area show a clear decreasing trend when going further back in time (fig. 14, see appendix A2 for dating details). When extrapolating to the bottom of a peat profile in order to obtain an initiation age, the accumulation rate of the above-lying part of the peat profile is used to extrapolate over the lowest part of the profile, which is older and has a lower fraction of remaining peat mass. As a result, these extrapolated ages will be biased towards younger basal ages. This effect increases with increasing distance between the bottom of the peat profile and the deepest radiocarbon date. When excluding the extrapolated basal ages from the analysis, the probability density function shifts towards older ages, clustering between 11.25 ka BP and 4.25 ka BP and corresponding much better with the probability density function of the model simulations (fig. 9). Here, both the radiocarbon dates as well as the model simulations show peaks in peat growth initiation in the periods 10.25 – 8.25 ka BP and 7.75 – 6.25 ka BP, which coincide with the periods of temperature increase. Overall, the simulations show broadly the same pattern as the radiocarbon dates, but with a more pronounced difference between periods. The spikes in the simulated initiation dates might be attributed to the use of a single set of parameter values for the entire study area resulting in a relatively similar response of many model gridpoints to the changing environmental conditions during the early-Holocene. The more diffuse probability density function for the radiocarbon dates might thus, at least partially, be ascribed to local heterogeneity. Additionally, as the available basal radiocarbon dates come from areas all over Scotland, the probability density curve is likely to include regional differences in peatland initiation ages as well.



415 **Figure 14: Reconstructed peat accumulation rates based on all available radiocarbon dates within the study area and mean peat accumulation rate .**



A study for the British Isles based on an envelope climate model for blanket peatlands finds a contraction in the area suitable for blanket peatland development in eastern Scotland since 6 ka BP and other studies find post-6 ka accumulation rates to be relatively low (Simmons and Innes, 1988). In this study, accumulation rates decrease from 8 ka to 6 ka BP onwards (fig. 7).
420 Overall, the mean accumulation rate remains positive until approximately 2 ka BP, but never reaches the high values which occurred during the early Holocene. This results in a slowdown in the peatland development and carbon storage after 6 ka BP (fig. 8). The conclusion that the blanket peatland development in the Upper Dee area can be attributed to a climate warming, independent of an increase in precipitation, as demonstrated by the sensitivity analysis, is in line with a study by a Morris et al., who compared a large dataset of peatland initiation dates across the globe with GCM paleoclimate simulations, concluding
425 that peatland initiation in formerly glaciated areas can be attributed to rising growing season temperatures (Morris et al., 2018). Additionally, a recent study on buried peat layers indicates that in northern latitudes (>40°N) peat growth is extensive during warm periods such as the last interglacial and the MIS 3 interstadial (57 - 29 ka) (Treat et al., 2019). It is clear that anaerobic conditions are required for the development of peat soils. However, regional climatic changes towards wetter conditions do not seem to be necessary for blanket peatland initiation. Apparently, local factors driving the hydrology such as hillslope
430 topography, soil properties, etc. will determine where anoxic conditions will establish to enable blanket peatlands to develop (Morris et al., 2018).

The model simulations do not support the original hypothesis on the origin of the blanket peatlands, linking the peatland development to a deforestation-driven change in hillslope hydrology (Moore, 1973). Firstly, both the available basal radiocarbon dates and the simulated initiation dates indicate a shift towards peat soils during a period of increasing or stable
435 woodland cover (fig. 5, fig. 9). Secondly, the parameter sensitivity analysis indicates that a decrease in tree cover, either by natural or anthropogenic causes, decreases the peat growth potential because the decrease in evapotranspiration due to a loss of tree cover is outweighed by the reduction in biomass production under the environmental conditions present in the study area. Tipping (2008) studied the Holocene blanket peatland development in five upland and northern sites in Scotland using a combination of geomorphic, archaeological and radiocarbon data, resulting in the hypothesis that blanket peatlands were
440 common over large parts of the Scottish Highlands within the first few millennia of the Holocene either due to rapid soil development or by climatic changes (Tipping, 2008). This study supports the hypothesis of Tipping, as shown by the model simulations and peatland initiation dates and provides evidence that a changing climate (increasing mean annual temperature) was the main driver of blanket peatland development.

Although the simulated mean peat accumulation rates remain at low levels after 6 ka BP, this does not mean peat profiles are
445 unable to develop but rather that the peatlands at landscape scale are in dynamic equilibrium with the stabilising Holocene climate. This can be demonstrated using a forced model simulation where all peat soils are removed at 6 ka BP. The resultant simulated peat thickness evolution indicates that peat starts to develop immediately after the peat removal (fig. 15). After approximately 1500 years, the mean peat thickness over the study area reaches again the values of the standard model run. This indicates that the model can simulate peatland regeneration at locations which are impacted by a removal of the peat
450 cover either by natural processes (e.g. by shallow mass movements, gullies) or following anthropogenic peat cutting.

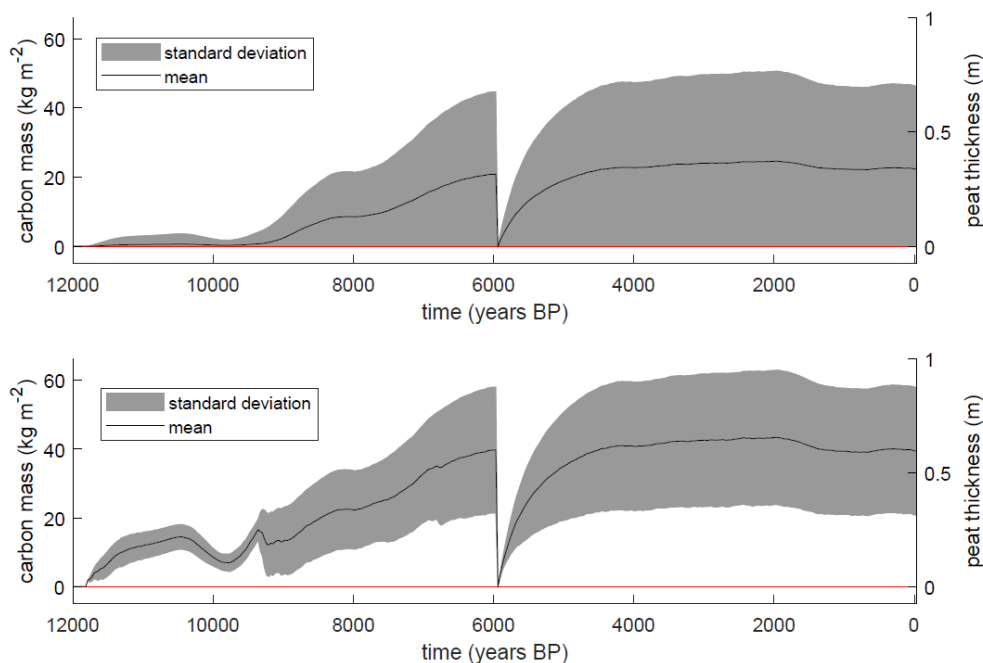


Figure 15: Simulated mean peat thickness/carbon mass and standard deviation for all gridpoints (top) and for the gridpoints with a peat cover (bottom), with a removal of all peat cover within the study area at 6 ka BP.

5 Conclusion

455 A new process-based model was presented to study long-term blanket peatland development along hillslopes. The simulations
for the past 12,000 years indicate that a relatively simple diplotelmic model is able to capture long-term peatland dynamics on
the landscape scale. However, point-by-point comparison still holds poor results, which can be attributed to the use of a single
set of calibrated parameters and the idealised representation of the model domain. Overall, both the field data and model
simulations indicate that the blanket peatlands in the Upper Dee area developed mostly during the Atlantic period, with a peak
460 in peat growth initiation dates around 9 ka BP. The timing of peatland initiation together with the results of the sensitivity
analysis support the hypothesis of a climate-driven origin of the blanket peatlands in the Scottish highlands, where the peatland
development shows to be driven by a long-term regional warming trend during the early-Holocene. A higher woodland cover
leads to an increase in peat growth potential, contradicting the original hypothesis of Moore (1973), which identified
deforestation as a potential driver of blanket peatland development. In more recent periods, the relatively stable climate and
465 land cover within the study area since 6 ka BP result in a stabilisation of the peatland development, indicating that the study
area served as a terrestrial carbon sink mainly during the Atlantic period and has stabilised during the late-Holocene.



Appendices

A1: MIDAS (Met office Integrated Data Archive System) weather stations used for the construction of the regression equations for orographic temperature and precipitation corrections.

Station name	MIDAS station code	Elevation (metres a.s.l.)	Latitude (degrees North)	Longitude (degrees West)
Braemar (irrigation farm)	14938	323	57.012	2.745
Dalwhinnie	14769	361	56.928	3.403
Corgarff	144	400	57.165	2.733
Forest Lodge No. 2	15190	305	56.847	3.001
Trinafour	15183	268	56.751	2.856
Glenshee Lodge	225	335	56.799	3.111
Pitcarmick	15251	198	56.694	2.627
Inschriach	14783	213	57.144	1.954

470



A2: Radiocarbon dating results. Calibrated ages were calculated using the Oxcal 4.3 software and the IntCal13 calibration curve (Bronk Ramsey, 2009; Reimer et al., 2013).

Sample ID	Lab-code	Conventional age (BP)	Calibrated age (cal a BP $\pm 1\sigma$)	Longitude (degrees)	Latitude (degrees)	Dated material	Sample depth (m)	Total peat depth (m)	Reference
DEEH1P3	RICH-26352	594 \pm 23 BP	599 \pm 26 cal a BP	-3.5117	56.9711	bulk peat	0.20	0.20	This study
Allt Connie H4P5-1	RICH-25414	941 \pm 27 BP	855 \pm 39 BP	-3.5667	56.9468	Plant remain	0.5	1.77	This study
Allt Connie H4P5-2	RICH-25429	2145 \pm 29 BP	2155 \pm 79 BP	-3.5667	56.9468	Bulk peat	1.03	1.77	This study
Allt Connie H4P5-3	RICH-25435	2899 \pm 30 BP	3036 \pm 52 BP	-3.5667	56.9468	Bulk peat	1.3	1.77	This study
Allt Connie H4P5-4	RICH-25415	3827 \pm 31 BP	4440 \pm 69 cal a BP	-3.5667	56.9468	bulk peat	1.70	1.77	This study
DEEH8P7	RICH-26330	2430 \pm 25 BP	2724 \pm 87 cal a BP	-3.6235	57.0005	bulk peat	0.65	0.71	This study
DEEH8P12-1	RICH-26327	2383 \pm 25 BP	2408 \pm 55 BP	-3.6258	56.9979	Bulk peat	0.51	0.94	This study
DEEH8P12-2	RICH-26349	4265 \pm 27 BP	5480 \pm 42 cal a BP	-3.6258	56.9979	bulk peat	0.86	0.94	This study
DEEH8P13-1	RICH-26350	4764 \pm 27 BP	5514 \pm 52 BP	-3.6265	56.9973	Bulk peat	1.06	1.40	This study
DEEH8P13-2	RICH-26329	7543 \pm 31 BP	11979 \pm 94 cal a BP	-3.6265	56.9973	bulk peat	1.21	1.40	This study
DEEH8P16	RICH-26334	6994 \pm 31 BP	9132 \pm 55 cal a BP	-3.6278	56.9958	wood	1.22	1.42	This study
DEEH9P7	RICH-26351	3241 \pm 25 BP	3649 \pm 40 cal a BP	-3.4847	57.0352	bulk peat	0.38	0.4	This study
DEEH10P8-1	RICH-26331	2333 \pm 25 BP	2347 \pm 20 BP	-3.4682	57.0499	Bulk peat	0.4	1.42	This study
DEEH10P8-2	RICH-26333	5184 \pm 28 BP	7324 \pm 51 cal a BP	-3.4682	57.0499	bulk peat	1.10	1.42	This study
DEEH13P7	RICH-26324	7350 \pm 30 BP	8287 \pm 60 cal a BP	-3.5606	56.9251	bulk peat	1.77	1.80	This study
DEEH15P1	RICH-26326	3865 \pm 24 BP	4633 \pm 60 cal a BP	-3.5305	56.9106	wood	1.33	1.43	This study
DEEH23P13-1	RICH-26328	2756 \pm 25 BP	2842 \pm 36 BP	-3.5656	57.0686	Bulk peat	0.75	2.34	This study
DEEH23P13-2	RICH-26332	4461 \pm 27 BP	5137 \pm 97 BP	-3.5656	57.0686	Bulk peat	1.5	2.34	This study
DEEH23P13-3	RICH-26335	9029 \pm 39 BP	10697 \pm 33 cal a BP	-3.5656	57.0686	bulk peat	2.29	2.34	This study
DEEH42P2	RICH-26325	3519 \pm 28 BP	3806 \pm 42 cal a BP	-3.3981	56.9023	bulk peat	1.99	2.00	This study
Allt Connie AC200-1	RICH-25434	528 \pm 28 BP	549 \pm 33 BP	-3.5648	56.9451	Bulk peat	0.47	1.59	This study
Allt Connie AC200-2	RICH-25430	1939 \pm 29 BP	1888 \pm 35 BP	-3.5648	56.9451	Bulk peat	1.02	1.59	This study
Allt Connie AC200-3	RICH-25433	3882 \pm 31 BP	4455 \pm 114 cal a BP	-3.5648	56.9451	wood	1.58	1.59	This study
Bynack Burn pollen core-1	RICH-22684	1570 \pm 31 BP	1466 \pm 40 BP	-3.6689	56.9497	Bulk peat	1.08	2.77	(Hunter, 2016)
Bynack Burn pollen core-2	RICH-22690	2008 \pm 28 BP	1956 \pm 35 BP	-3.6689	56.9497	Bulk peat	2.16	2.77	(Hunter, 2016)
Bynack Burn pollen core-3	RICH-22687	3006 \pm 34 BP	3409 \pm 76 cal a BP	-3.6689	56.9497	bulk peat	2.68	2.77	(Hunter, 2016)
Geldie Burn pollen core-1	RICH-22689	1688 \pm 28 BP	1598 \pm 40 BP	-3.6667	56.9789	Bulk peat	1.00	3.14	(Hunter, 2016)
Geldie Burn pollen core-2	RICH-22685	3729 \pm 33 BP	4073 \pm 59 BP	-3.6667	56.9789	Bulk peat	2.00	3.14	(Hunter, 2016)
Geldie Burn pollen core-3	RICH-22686	5510 \pm 38 BP	6580 \pm 48 cal a BP	-3.6667	56.9789	bulk peat	3.02	3.14	(Hunter, 2016)
Geldie Lodge pollen core-1	GU-17252	2880 \pm 35 BP	3010 \pm 58 BP	-3.7181	56.9625	Bulk peat	0.51	1.48	(Paterson, 2011)
Geldie Lodge pollen core-2	GU-17254	5540 \pm 35 BP	7745 \pm 64 cal a BP	-3.7181	56.9625	bulk peat	1.43	1.48	(Paterson, 2011)
Luibeg H200-1	RICH-25412	386 \pm 26 BP	437 \pm 59 BP	-3.6457	57.0444	Plant remain	0.5	1.50	This study
Luibeg H200-2	RICH-25427	1200 \pm 28 BP	1127 \pm 45 BP	-3.6457	57.0444	Plant remain	1.06	1.50	This study
Luibeg H200-3	RICH-25436	3603 \pm 32 BP	4411 \pm 113 cal a BP	-3.6456	57.0444	bulk peat	1.45	1.50	This study



Author contribution

The conceptualisation and methodology development of this project was carried out by WS, NB and GV. The field work was performed by WS, NB and GV. WS carried out the lab work, developed the model code and performed the model simulations.
480 GV and NB supervised the research. The writing of the manuscript was carried out by WS, NB and GV.

Competing interests

The authors declare that they have no conflict of interest.

Acknowledgements

Ward Swinnen holds a PhD grant of the FWO – Research Foundation Flanders (application 1167019N). This research is part
485 of a project funded by the FWO (application G0A6317N). The authors thank Mar estate, Mar lodge estate and Invercauld
estate for the permission to access the area. The authors thank Teun Daniëls, Sofie De Geeter, Yasmine Hunter, Ellen Jennen,
Vincent Lenaerts and Remi Swinnen for their assistance during the field campaigns. Danny Paterson and Richard Tipping are
thanked for sharing their pollen data from the Upper Dee catchment. Pollen data of Birks (1969) and Huntley (1994) were
extracted from the European Pollen Database (EPD; <http://www.europeanpollendatabase.net/>) and the work of the data
490 contributors and the EPD community is gratefully acknowledged.

References

- Baird, A. J., Morris, P. J. and Belyea, L. R.: The DigiBog peatland development model 1: rationale, conceptual model, and hydrological basis, *Ecohydrology*, 5, 242–255, doi:10.1002/eco.2, 2012.
- Ballantyne, C. K.: After the ice: Holocene geomorphic activity in the Scottish Highlands, *Scottish Geogr. J.*, 124(1), 8–52,
495 doi:10.1080/14702540802300167, 2008.
- Ballard, C. E., McIntyre, N., Wheeler, H. S., Holden, J. and Wallage, Z. E.: Hydrological modelling of drained blanket peatland, *J. Hydrol.*, 407(1–4), 81–93, doi:10.1016/j.jhydrol.2011.07.005, 2011.
- Beilman, D. W. and Yu, Z.: Differential Response of Peatland Types to Climate: Modeling Peat Accumulation in Continental Western Canada., 2001.
- 500 Belyea, L. R. and Malmer, N.: Carbon sequestration in peatland : patterns and mechanisms of response to climate change, *Glob. Chang. Biol.*, 10, 1043–1052, doi:10.1111/j.1365-2486.2004.00783.x, 2004.
- Birks, H. H.: *Studies in the vegetational history of Scotland.*, University of Cambridge., 1969.
- Blaauw, M.: Methods and code for “classical” age-modelling of radiocarbon sequences, *Quat. Geochronol.*, 5(5), 512–518, doi:10.1016/j.quageo.2010.01.002, 2010.



- 505 Bronk Ramsey, C.: Bayesian Analysis of Radiocarbon Dates, *Radiocarbon*, 51(01), 337–360, doi:10.1017/S0033822200033865, 2009.
- Cairns, A., Dutch, M. E., Guy, E. M. and Stout, J. D.: Effect of irrigation with municipal water or sewage effluent on the biology of soil cores: I. Introduction, total microbial populations, and respiratory activity, *New Zeal. J. Agric. Res.*, 21(1), 1–9, doi:10.1080/00288233.1978.10427377, 1978.
- 510 Chapman, S. J. and Thurlow, M.: Peat respiration at low temperatures, *Soil Biol. Biochem.*, 30(8–9), 1013–1021, doi:10.1016/S0038-0717(98)00009-1, 1998.
- Clymo, R. S.: The Limits to Peat Bog Growth, *Philos. Trans. R. Soc. B Biol. Sci.*, 303(1117), 605–654, doi:10.1098/rstb.1984.0002, 1984.
- Cunliffe, A. M., Baird, A. J. and Holden, J.: Hydrological hotspots in blanket peatlands: Spatial variation in peat permeability around a natural soil pipe, *Water Resour. Res.*, 49(9), 5342–5354, doi:10.1002/wrcr.20435, 2013.
- 515 Dai, T. S. and Sparling, J. H.: Measurement of hydraulic conductivity of peats, *Can. J. Soil Sci.*, 53, 21–26, 1973.
- Dunn, S. M., Langan, S. J. and Colohan, R. J. E.: The impact of variable snow pack accumulation on a major Scottish water resource, *Sci. Total Environ.*, 265(1–3), 181–194, doi:10.1016/S0048-9697(00)00658-6, 2001.
- Ellis, C. J. and Tallis, J. H.: Climatic control of blanket mire development at Kentra Moss, north-west Scotland, *J. Ecol.*, 88(5), 869–889, doi:10.1046/j.1365-2745.2000.00495.x, 2000.
- 520 Everest, J. and Kubik, P.: The deglaciation of eastern Scotland: Cosmogenic ^{10}Be evidence for a Lateglacial stillstand, *J. Quat. Sci.*, 21(1), 95–104, doi:10.1002/jqs.961, 2006.
- Frolking, S., Roulet, N. T., Tuittila, E., Bubier, J. L., Quillet, A., Talbot, J. and Richard, P. J. H.: A new model of Holocene peatland net primary production, decomposition, water balance, and peat accumulation, *Earth Syst. Dyn.*, 1(1), 1–21, doi:10.5194/esd-1-1-2010, 2010.
- 525 Fyfe, R. M., Twiddle, C., Sugita, S., Gaillard, M. J., Barratt, P., Caseldine, C. J., Dodson, J., Edwards, K. J., Farrell, M., Froyd, C., Grant, M. J., Huckerby, E., Innes, J. B., Shaw, H. and Waller, M.: The Holocene vegetation cover of Britain and Ireland: Overcoming problems of scale and discerning patterns of openness, *Quat. Sci. Rev.*, 73, 132–148, doi:10.1016/j.quascirev.2013.05.014, 2013.
- 530 Gallego-Sala, A. V., Charman, D. J., Harrison, S. P., Li, G. and Prentice, I. C.: Climate-driven expansion of blanket bogs in Britain during the Holocene, *Clim. Past*, 12(1), 129–136, doi:10.5194/cp-12-129-2016, 2016.
- Gallego-sala, A. V and Prentice, I. C.: Blanket peat biome endangered by climate change, *Nat. Clim. Chang.*, 3, 152–155, doi:10.1038/nclimate1672, 2013.
- Garnett, M. H.: Carbon storage in Pennine moorland and response to change, University of Newcastle-Upon_tyne., 1998.
- 535 Gorham, E.: Northern Peatlands : Role in the Carbon Cycle and Probable Responses to Climatic Warming, *Ecol. Appl.*, 1(2), 182–195, 1991.
- Hilbert, D. W., Roulet, N. and Moore, T.: Modelling and analysis of peatlands as dynamical systems, *J. Ecol.*, 88, 230–242, 2000.



- Hilberts, A. G. J., van Loon, E. E., Troch, P. A. and Paniconi, C.: The hillslope-storage Boussinesq model for non-constant
540 bedrock slope, *J. Hydrol.*, 291(3–4), 160–173, doi:10.1016/J.JHYDROL.2003.12.043, 2004.
- Holden, J. and Burt, T. P.: Infiltration, runoff and sediment production in blanket peat catchments: Implications of field rainfall
simulation experiments, *Hydrol. Process.*, 16(13), 2537–2557, doi:10.1002/hyp.1014, 2002.
- Holden, J. and Burt, T. P.: Hydraulic conductivity in upland blanket peat: measurement and variability, *Hydrol. Process.*,
17(2003), 1227–1237, doi:10.1002/hyp.1182, 2003.
- 545 Holden, J., Wallage, Z. E., Lane, S. N. and McDonald, A. T.: Water table dynamics in undisturbed, drained and restored
blanket peat, *J. Hydrol.*, 402(1–2), 103–114, doi:10.1016/j.jhydrol.2011.03.010, 2011.
- Huang, C. C.: Holocene landscape development and human impact in the Connemara Uplands, Western Ireland, *J. Biogeogr.*,
29, 153–165, 2002.
- Hunter, Y.: A Holocene paleo-ecological analysis of peat stratigraphy in the Upper-Dee valley (Scotland) and the Dijle
550 catchment (Belgium)., MSc thesis, Department of Earth and Environmental Science, KU Leuven., 2016.
- Huntley, B.: Late Devensian and Holocene palaeoecology and palaeoenvironments of the Morrone Birkwoods, Aberdeenshire,
Scotland., *J. Quat. Sci.*, 9(4), 311–336, 1994.
- Ingram, H. A. P.: Hydrology, in *Mires: Swamp, Bog, Fen and Moor. A. General Studies*, edited by A. J. P. Gore, pp. 67–158,
Elsevier Scientific Publishing Company, Amsterdam., 1983.
- 555 Jones, P. S., Stevens, D. P., Blackstock, T. H., Burrows, C. R. and Howe, E. A., Eds.: *Priority Habitats of Wales: A Technical
Guide*, Bangor., 2003.
- Kleinen, T., Brovkin, V. and Schuldt, R. J.: A dynamic model of wetland extent and peat accumulation: Results for the
Holocene, *Biogeosciences*, 9(1), 235–248, doi:10.5194/bg-9-235-2012, 2012.
- Lafleur, P. M., Hember, R. A., Admiral, S. W. and Roulet, N. T.: Annual and seasonal variability in evapotranspiration and
560 water table at a shrub-covered bog in southern Ontario, Canada, *Hydrol. Process.*, 19(18), 3533–3550, doi:10.1002/hyp.5842,
2005.
- Lucchese, M., Waddington, J. M., Poulin, M., Pouliot, R., Rochefort, L. and Strack, M.: Organic matter accumulation in a
restored peatland: Evaluating restoration success, *Ecol. Eng.*, 36, 482–488, doi:10.1016/j.ecoleng.2009.11.017, 2010.
- Maizels, J.: The physical background of the River Dee, in *The biology and management of the river Dee*, edited by D. Jenkins,
565 pp. 7–22, Huntingdon., 1985.
- Malmer, N. and Wallen, B.: Input rates, decay losses and accumulation rates of carbon in bogs during the last millennium:
internal processes and environmental changes, , 14(1), 111–117, 2004.
- Maurer, E.: Spatial variation in organic carbon storage in Holocene floodplain soils. Msc thesis, Department of Earth and
Environmental Science, KU Leuven, 132, 2015.
- 570 Mauri, A., Davis, B. A. S., Collins, P. M. and Kaplan, J. O.: The climate of Europe during the Holocene: A gridded pollen-
based reconstruction and its multi-proxy evaluation, *Quat. Sci. Rev.*, 112, 109–127, doi:10.1016/j.quascirev.2015.01.013,
2015.



- Mazier, F., Gaillard, M. J., Kuneš, P., Sugita, S., Trondman, A. K. and Broström, A.: Testing the effect of site selection and parameter setting on REVEALS-model estimates of plant abundance using the Czech Quaternary Palynological Database, 575 *Rev. Palaeobot. Palynol.*, 187, 38–49, doi:10.1016/j.revpalbo.2012.07.017, 2012.
- MetOffice: Met Office Integrated Data Archive System (MIDAS) Land and Marine Surface Stations Data (1853-current)., [online] Available from: <http://catalogue.ceda.ac.uk/uuid/220a65615218d5c9cc9e4785a3234bd0> (Accessed 16 January 2019), 2012.
- Moore, P. D.: The Influence of Prehistoric Cultures upon the Initiation and Spread of Blanket Bog in Upland Wales, *Nature*, 580 241, 350–353, 1973.
- Morris, P. J., Baird, A. J. and Belyea, L. R.: The DigiBog peatland development model 2: ecohydrological simulations in 2D, *Ecohydrology*, 5, 256–268, doi:10.1002/eco.2, 2012.
- Morris, P. J., Swindles, G. T., Valdes, P. J., Ivanovic, R. F., Gregoire, L. J., Smith, M. W., Tarasov, L., Haywood, A. M. and Bacon, K. L.: Global peatland initiation driven by regionally asynchronous warming, , 1–6, doi:10.1073/pnas.1717838115, 585 2018.
- Parry, L. E., Charman, D. J. and Noades, J. P. W.: A method for modelling peat depth in blanket peatlands, *Soil Use Manag.*, 28(4), 614–624, doi:10.1111/j.1475-2743.2012.00447.x, 2012.
- Paterson, D.: The Holocene history of *Pinus sylvestris* woodland in the Mar Lodge Estate , Cairngorms , Eastern Scotland, PhD thesis, Institute of Natural Sciences, University of Stirling, 2011.
- 590 Peeters, I., Rommens, T., Verstraeten, G., Govers, G., Van Rompaey, A., Poesen, J. and Van Oost, K.: Reconstructing ancient topography through erosion modelling, *Geomorphology*, 78(3–4), 250–264, doi:10.1016/j.geomorph.2006.01.033, 2006.
- Reimer, P. J., Bard, E., Bayliss, A., Beck, J. W., Blackwell, P. G., Ramsey, C. B., Buck, C. E., Cheng, H., Edwards, R. L., Friedrich, M., Grootes, P. M., Guilderson, T. P., Haflidason, H., Hajdas, I., Hatté, C., Heaton, T. J., Hoffmann, D. L., Hogg, A. G., Hughen, K. A., Kaiser, K. F., Kromer, B., Manning, S. W., Niu, M., Reimer, R. W., Richards, D. A., Scott, E. M., 595 Southon, J. R., Staff, R. A., Turney, C. S. M. and van der Plicht, J.: IntCal13 and Marine13 Radiocarbon Age Calibration Curves 0–50,000 Years cal BP, *Radiocarbon*, 55(04), 1869–1887, doi:10.2458/azu_js_rc.55.16947, 2013.
- Rosa, E. and Larocque, M.: Investigating peat hydrological properties using field and laboratory methods: application to the Lanoraie peatland complex (southern Quebec, Canada), *Hydrol. Process.*, 22(2008), 1866–1875, doi:10.1002/hyp, 2008.
- Rosswall, T.: Decomposition of plant litter at Stordalen - a summary. In: International Biological Programme: Swedish tundra 600 biome progress report 1973., 1973.
- Simmons, I. G. and Innes, J. B.: Late Quaternary vegetational history of the North York Moors. VIII. Correlation of Flandrian II litho- and pollen stratigraphy at North Gill, Glaisdale Moor, *J. Biogeogr.*, 15, 249–272, 1988.
- Smith, J. S.: Land use within the catchment of the river Dee, in *The biology and management of the river Dee*, edited by D. Jenkins, pp. 29–33, Huntingdon., 1985.
- 605 Sugita, S.: Theory of quantitative reconstruction of vegetation I: Pollen from large sites REVEALS regional vegetation composition, *Holocene*, 17(2), 229–241, doi:10.1177/0959683607075837, 2007.



- Szumigalski, A. R. and Bayley, S. E.: Net aboveground primary production along a peatland gradient in central Alberta in relation to environmental factors, *Ecoscience*, 4(3), 385–393, doi:10.1080/11956860.1997.11682417, 1997.
- 610 Tetzlaff, D. and Soulsby, C.: Sources of baseflow in larger catchments - Using tracers to develop a holistic understanding of runoff generation, *J. Hydrol.*, 359(3–4), 287–302, doi:10.1016/j.jhydrol.2008.07.008, 2008.
- Tipping, R.: Blanket peat in the Scottish Highlands: Timing, cause, spread and the myth of environmental determinism, *Biodivers. Conserv.*, 17(9), 2097–2113, doi:10.1007/s10531-007-9220-4, 2008.
- Treat, C. C., Kleinen, T., Broothaerts, N., Dalton, A. S., Dommain, R., Douglas, T. A., Drexler, J. Z., Finkelstein, S. A., Grosse, G., Hope, G., Hutchings, J., Jones, M. C., Kuhry, P., Lacourse, T., Lähteenoja, O., Loisel, J., Notebaert, B., Payne, R. J., Peteet, 615 D. M., Sannel, A. B. K., Stelling, J. M., Strauss, J., Swindles, G. T., Talbot, J., Tarnocai, C., Verstraeten, G., Williams, C. J., Xia, Z., Yu, Z., Välijanta, M., Hättestrand, M., Alexanderson, H. and Brovkin, V.: Widespread global peatland establishment and persistence over the last 130,000 y, *Proc. Natl. Acad. Sci.*, 116(11), 4822–4827, doi:10.1073/pnas.1813305116, 2019.
- Trondman, A. K., Gaillard, M. J., Sugita, S., Björkman, L., Greisman, A., Hultberg, T., Lagerås, P., Lindbladh, M. and Mazier, F.: Are pollen records from small sites appropriate for REVEALS model-based quantitative reconstructions of past regional 620 vegetation? An empirical test in southern Sweden, *Veg. Hist. Archaeobot.*, 25(2), 131–151, doi:10.1007/s00334-015-0536-9, 2016.
- Warren, G., Fraser, S., Clarke, A., Driscoll, K., Mitchell, W., Noble, G., Paterson, D., Schulting, R., Tipping, R., Verbaas, A., Wilson, C. and Wickham-Jones, C.: Little House in the Mountains? A small Mesolithic structure from the Cairngorm Mountains, Scotland, *J. Archaeol. Sci. Reports*, (November 2017), 0–1, doi:10.1016/j.jasrep.2017.11.021, 2018.
- 625 Williams, J. R., Dyke, P. T. and Jones, C. A.: EPIC - A model for assessing the effects of erosion on soil productivity, in *Analysis of Ecological Systems: State-of-the-Art in Ecological Modelling*, edited by W. K. Lauenroth, G. V. Skogerboe, and M. Flug, p. 971, Elsevier., 1983.
- Wu, J.: Response of peatland development and carbon cycling to climate change: A dynamic system modeling approach, *Environ. Earth Sci.*, 65(1), 141–151, doi:10.1007/s12665-011-1073-1, 2012.
- 630 Xu, J., Morris, P. J., Liu, J. and Holden, J.: PEATMAP: Refining estimates of global peatland distribution based on a meta-analysis, *Catena*, 160(April 2017), 134–140, doi:10.1016/j.catena.2017.09.010, 2018.
- Yu, Z., Turetsky, M. R., Campbell, I. D. and Vitt, D. H.: Modelling long-term peatland dynamics. II. Processes and rates as inferred from litter and peat-core data, *Ecol. Modell.*, 145(2–3), 159–173, doi:10.1016/S0304-3800(01)00387-8, 2001.
- 635 Yu, Z., Beilman, D. W., Frohling, S., MacDonald, G. M., Roulet, N. T., Camill, P. and Charman, D. J.: Peatlands and Their Role in the Global Carbon Cycle, *Eos, Trans. Am. Geophys. Union*, 92(12), 97, doi:10.1029/2011EO120001, 2011.